Accepted Manuscript

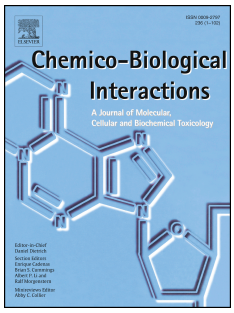

8-Cetylcoptisine, a new coptisine derivative, induces mitochondria-dependent apoptosis and G0/G1 cell cycle arrest in human A549□cells

Bing Han, Pu Jiang, Heshan Xu, Wuyang Liu, Jian Zhang, Siqi Wu, Liangyu Liu, Wenyu Ma, Xuegang Li, Xiaoli Ye

PII: S0009-2797(18)31041-X

DOI: https://doi.org/10.1016/j.cbi.2018.11.005

Reference: CBI 8456

To appear in: *Chemico-Biological Interactions*

Received Date: 5 August 2018

Revised Date: 31 October 2018

Accepted Date: 12 November 2018

Please cite this article as: B. Han, P. Jiang, H. Xu, W. Liu, J. Zhang, S. Wu, L. Liu, W. Ma, X. Li, X. Ye, 8-Cetylcoptisine, a new coptisine derivative, induces mitochondria-dependent apoptosis and G0/G1 cell cycle arrest in human A549□cells, *Chemico-Biological Interactions* (2018), doi: https://doi.org/10.1016/j.cbi.2018.11.005.

Graphical abstract

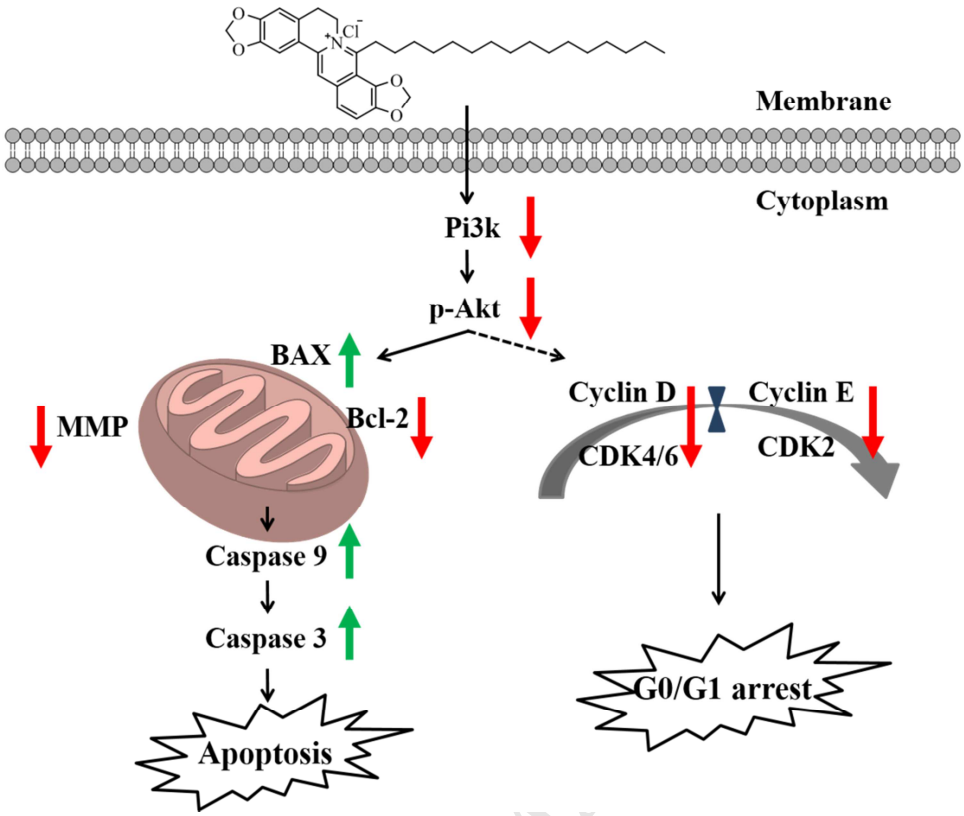

8-Cetylcoptisine, a new coptisine derivative, induces mitochondria-dependent apoptosis and G0/G1 cell cycle arrest in human A549 cells

Bing Han[a,†], Pu Jiang[a,†], Heshan Xu[b], Wuyang Liu[a], Jian Zhang[b], Siqi Wu[a], Liangyu Liu[a], Wenyu Ma[b], Xuegang Li[a,c,]*, Xiaoli Ye[b,c,]**

[a] Chongqing productivity promotion center for the modernization of Chinese traditional medicine, School of Pharmaceutical Sciences, Southwest University, Chongqing, 400716, China

[b] School of Life Sciences, Southwest University, Chongqing, 400715, China

[c] Chongqing Engineering Research Center for Pharmaceutical Process and Quality Control, Chongqing, 400716, China

**Correspondence to*: X. Li, School of Pharmaceutical Sciences, Southwest University, Tiansheng Road 2, Beibei district, Chongqing, 400715, China. Tel./fax: +86 023-68250728.

***Correspondence to*: X. Ye, School of Life Sciences, Southwest University, Tiansheng Road 2, Beibei district, Chongqing, 400715, China. Tel./fax: +86 023-68250728.

E-mail addresses: Xuegangli@swu.edu.cn (X. Li), yexiaoli@swu.edu.cn (X. Ye).

[†]These authors contributed equally to this work.

Abstract

Lung cancer is the worldwide leading cause of cancer-related death. Here, we described the synthesis and the anticancer activity of a novel coptisine derivative 8-cetylcoptisine (CCOP) on lung carcinoma *in vitro* and *in vivo*. CCOP inhibited the cell viability of A549, BGC-823, MDA-MB-231, HCT-116 and HepG2 cell lines. In A549 cells, CCOP induced apoptosis, G0/G1 cell cycle arrest and decreased mitochondrial membrane potential (MMP) in a dose-dependent manner. Western blot analysis showed that CCOP increased the expression of Bcl-2-associated X protein (Bax), cleaved caspase 3 and 9, while decreased B-cell lymphoma 2 (Bcl-2), cyclins D and E, cyclin dependent kinases (CDKs) 2, 4 and 6, along with the inactivation of the upstream phosphoinositide 3-kinase (Pi3k)/protein kinase B (Akt) signaling. Further *in vivo* studies showed that CCOP (10 mg/kg) significantly delayed tumor growth in A549 xenograft nude mice, which is stronger than that of coptisine (100 mg/kg). These data suggested that CCOP could be a candidate for lung cancer therapy.

Keywords: coptisine derivative; 8-cetylcoptisine; lung cancer; apoptosis; cell cycle

Abbreviations

Akt, protein kinase B; AO/EB, acridine orange/ethidium bromide; Bak, Bcl-2 homologous antagonist/killer; Bax, Bcl-2-associated X protein; Bcl-2, B-cell lymphoma 2; CCOP, 8-cetylcoptisine; CDKs, cyclin dependent kinases; COP, coptisine; $DiOC_6(3)$, 3,3'-dihexyloxacarbocyanine iodide; DMEM, Dulbecco's

Modified Eagle's Medium; MMP, mitochondrial membrane potential; MOMP, mitochondrial outer membrane permeabilization; NSCLC, non-small-cell lung cancer; PARP, poly ADP-ribose polymerase; PI, propidium iodide; Pi3k, phosphoinositide 3-kinase.

1. Introduction

Lung cancer is the leading cause of cancer incidence and mortality worldwide. According to International Agency for Research on Cancer, about 2.1 million new cases and 1.8 million deaths are predicted in 2018 [1]. Non-small-cell lung cancer (NSCLC) accounts for almost 80% of lung cancer cases. In recent years, the combined use of chemotherapy and surgery has led to the improvement of patient's outcomes. However, the 5-year survival rate of lung cancer remains disappointing [2], suggesting the need for the development of novel therapeutic strategies for lung cancer treatment.

Apoptosis, also called programmed cell death, plays a critical role in the pathogenesis of lung cancer. Numerous chemotherapeutic agents are reported to induce death in cancer cells by apoptosis [3, 4]. It is well established that caspase proteins are key modulators of apoptosis induction [5]. Upon activation, initiator caspases 8 and 9 cleave and activate downstream effector caspases 3, 6, and 7, which further execute apoptosis by cleaving target proteins such as poly ADP-ribose polymerase (PARP) [6]. On the other hand, the B-cell lymphoma 2 (Bcl-2) family proteins such as Bcl-2 and Bcl-2-associated X protein (Bax) regulate the mitochondrial outer membrane permeabilization (MOMP) and activate mitochondrial-mediated apoptosis pathway [7]. Dysregulation of phosphoinositide 3-kinase (Pi3k)/protein kinase B (Akt) components promotes pro-apoptotic function of Bax and induces mitochondrial membrane potential (MMP) reduction and reactive oxygen species production [8]. Besides, Pi3k/Akt pathway triggers a network positively regulates cell cycle transition

which relies on the activation of a series of cyclins and cyclin dependent kinases (CDKs) [9]. Inhibition function of CDKs 2, 4, 6 and cyclins D, E could induce G1/S arrest [10], while down-regulation of CDK 1 and cyclin B1 induces G2/M arrest [11]. Thus, the inhibition of Pi3k/Akt signaling may be a target for human cancer treatment [12].

Natural products are considered an important source of anticancer agents, for example, paclitaxel from *Taxus brevifolia*, and camptothecin from *Camptotheca acuminata* [13, 14]. It has been reported that the antitumor activity of coptisine (COP) from *Coptis chinensis* Franch (*Ranunculaceae*) against lung [15], colon [16, 17], liver [18], breast [19] and bone cancer [20]. However, its usage is limited because of poor bioavailability, e.g. the absolute bioavailability of COP is between 1.87% to 0.52% [21]. Alkylation is frequently used for structural modification of natural products which may enhance the bioavailability and activity [22]. Hu *et al*. reported that adding an hexadecyl moiety to the C8 of berberine, an analogue of COP, increased the maximal plasma concentration (C_{max}) by 2.8-fold. The relative bioavailability of berberine to the derivative was 7.7% [23]. In addition, Jiang *et al*. reported that adding C4, C6, C8, C10 and C12 alkyl chain at C8 of COP inhibited proliferation and enhanced the glucose-lowering effect in HepG2 cells [24]. Besides, 8-octylcoptisine exhibited higher antimicrobial activity than COP, especially against gram positive bacteria [25]. Based on this, we synthesized a new COP derivative 8-cetylcoptisine (CCOP) and investigated the potential antitumor effect on lung cancer *in vitro* and *in vivo*.

2. Material and methods

2.1. Compound and reagents

CCOP was synthesized as shown in Scheme 1 [22]. Grignard reagents were prepared from Mg ribbon (44 mmol) and hexadecyl bromate (40 mmol) in absolute THF (100 ml). To a mixture of Grignard reagents in absolute THF, the suspension of compound 1 (30 mmol) was added drop-wisely. The reaction mixture was stirred under N_2 at 0ºC for 1 h. After warming at room temperature, the solution was heated to reflux for 1 h. Then the solvent was removed by evaporation, redissolved in ethyl acetate and recrystallized in MeOH to obtain compound 2. To a stirred solution of compound 2 (10 mmol) in hot AcOH (100 ml), Br_2 (10 mmol) was added drop-wisely and heated under reflux for 1 h. After cooling down at room temperature, the precipitate was filtered and washed with 10% $Na_2S_2O_5$ solution, then with H_2O and recrystallized in MeOH to yield compound 3. Then, compound 3 was solvated in hot MeOH, reacted with AgCl and recrystallized in MeOH at -20ºC to obtain compound 4. ^{1}H and ^{13}C NMR spectra were detected on a Bruker Ascend 400 spectrometer (Bruker Biospin, Switzerland). Mass spectrum was recorded on LCMS-8030 (Shimadzu, Japan).

COP (> 95% by HPLC) was prepared from the rhizome of *Coptis chinensis* Franch according to a previous method [26]. Antibodies against caspase 3, caspase 9, Bcl-2, Bax, CDK 2, CDK 4, CDK 6, Cyclin D, Cyclin E and anti-rabbit IgG HRP-conjugated secondary antibody were purchased from Proteintech Group Inc., China. Antibodies against Pi3k, Akt and β-actin were purchased from Bioss Biotechnology Inc., China. Antibody against p-Akt was purchased from Cell

Signaling Technology Inc., USA.

2.2. Cell culture

Human A549, BGC-823, MDA-MB-231, HCT-116 and HepG2 cells were obtained from Cell Bank of Chinese Academy of Sciences (Shanghai, China). All cells were cultured in Dulbecco's Modified Eagle's Medium (DMEM) containing 1% penicillin/streptomycin (Invitrogen, USA) and 10% fetal bovine serum (BBI life sciences, China). The cells were grown at 37°C in a 95% humidified atmosphere with 5% CO_2.

2.3. Cell viability assessment

Cell viability was determined by MTT (Sigma-Aldrich, USA) assay [13]. Briefly, cells were seeded in 96-well plate at 6×10^3 cell/well and incubated overnight. CCOP was dissolved in DMSO solution and added to the wells with the final concentrations of 0−2 μg/mL. After treated for 18 h, 20 μL MTT (0.5 mg/mL) was added to each well and treated for 4 h at 37°C. The supernatant was replaced with DMSO and measured at 490 nm. The cell viability was normalized to untreated cells.

2.4. Flow cytometry

Cells in log-phase growth were seeded at 2×10^5 cells/well. For apoptosis assay, cells were harvested, washed and stained with Annexin-V/propidium iodide (PI) kit (Sigma-Aldrich, USA) according to the manufacturer's instruction. For cell cycle assay, cells were fixed in 70% ethanol at 4°C overnight then stained with 40 μg/mL PI and detected by flow cytometer (BD FacsVerse, USA). The results were analyzed by Flow Jo software (Tree Star Inc., USA) [16].

2.5. Acridine orange/ethidium bromide (AO/EB) staining

For AO/EB staining, cells were seeded at 4×10^4/well on 12-well culture plate and treated with CCOP. After 24 h incubation, cells were harvest, resuspended and incubated in 4 μg/mL AO/EB for 1 min in the dark. Cells were imaged under a fluorescence microscope (Nikon Eclipse Ci, Japan). Red fluorescence represents apoptosis cells while green fluorescence represents healthy cells. At least 500 cells were counted and the apoptosis rate was calculated by the percentage of red fluorescence cells in all cells [27].

2.6. MMP assay

The MMP was detected with 3,3'-dihexyloxacarbocyanine iodide ($DiOC_6(3)$, Sigma-Aldrich, USA) as reported previously [28]. Lipophilic cation such as $DiOC_6(3)$ was transported and concentrated within the mitochondrial matrix by the negative membrane potential. After CCOP treatment, cells were incubated with 50 nM $DiOC_6(3)$ for 20 min at 37°C, rinsed with PBS and subsequently detected by flow cytometry (excitation 488 nm; emission 525 nm). The results were analyzed using Flow Jo software. Cells with lower fluorescence indicate loss of MMP.

2.7. Western blot analysis

Total protein was extracted by RIPA buffer (BBI life sciences, China) containing protease inhibitors, separated by 10−15% SDS-PAGE, and transferred into polyvinylidene fluoride membrane. After blocked by 10% nonfat milk for 2 h, antibodies against Pi3k, Akt, p-Akt, caspase 3, 9, Bcl-2, Bax, CDK 2, CDK 4, CDK 6, Cyclin D, Cyclin E and β-actin were incubated at 4ºC overnight. Subsequently, the

membranes were rinsed with TBST and incubated with anti-rabbit IgG HRP-conjugated secondary antibody at room temperature for 2 h. The results were visualized with ECL reagent (Bio-Rad, USA) and quantified using Image J software.

2.8. Immunohistochemistry studies

Paraffin-embedded tumor sections were dewaxed, rehydrated, antigen retrieval by 10 mM sodium citrate buffer (pH 6.0) at 98ºC for 15 min and endogenous peroxidase blocked with 3% H_2O_2 for 15 min. The slides were blocked with serum and incubated with Ki-67, cleaved caspase 3 and Bcl-2. After rinsed with PBS, the sections were incubated with IgG HRP-conjugated antibodies for 1 h at room temperature and further stained with 3, 3'-diaminobenzidine and haematoxylin solution. The images were captured under a microscope and analyzed using Image Pro Plus software [29].

2.9. Animal experiments

BALB/c nude mice (4-weeks old) were purchased from Beijing Huafukang Bioscience Co. Inc., China (permit number: SCXK-JING 2014-0004) and housed in sterile filter-topped cages. All animal experiments were in accordance with the Laboratory Animal Care and Use Committee of Southwest University (permit number: SCXK-YU 2014-0002). After 7 days acclimation, A549 cells were subcutaneously inoculated in the right foreleg (5×10^6 cells/mice, n = 5). The mice were treated with 5 mg/kg (CCOP-L), 10 mg/kg (CCOP-H) or 100 mg/kg (COP) by oral gavage for 25 days. Mice in normal control (NC) and tumor control (TC) groups were administered with saline. Tumor volume was measured using a caliper every two days and calculated as tumor length × tumor width^2/2. At the time of sacrificing, tumors and

other tissues were quickly dissected, weighed and stored at -80ºC.

2.10. Statistical analysis

All values were expressed as mean ± SD. Differences between groups were analyzed by one-way ANOVA using SPSS 20.0 software. Values at or below $p < 0.05$ were considered as significant.

3. Results

3.1. Synthesis and identification

The synthetic process and chemical structure of CCOP is shown in Scheme 1 and Fig. 1A. CCOP: $C_{35}H_{46}NO_4$, yellow powder (> 95% by HPLC, Fig. 1B). ^{13}C NMR (400 MHz, CD_3OD) δ: 14.41 (C-16'), 23.71 (C-15'), 28.28 (C-5), 29.27 (C-3'), 30.25 (C-4'), 30.45 (C-5'), 30.61 (C-6'), 30.69 (C-7'), 30.74 (C8'-C13'), 30.77 (C-14'), 33.06 (C-2'), 33.35 (C-1'), 50.97 (C-6), 103.57 (-OCH_2O-), 104.96 (-OCH_2O-), 106.84(C-1), 108.68 (C-4), 115.28 (C-8a), 121.47 (C-11), 121.77 (C-13b), 122.91 (C-13), 124.24 (C-12), 131.86 (C-4a), 134.07 (C-12a), 139.49 (C-13a), 145.89 (C-9), 149.74 (C-8), 149.88 (C-10), 151.88 (C-2), 161.76 (C-3). ^1H NMR (400 MHz, CD_3OD) δ: 0.90 (t, J = 6 Hz, 3 H, 16'-CH_3), 1.29 [m, 24 H, -$(CH_2)_{12}$-], 1.46 (m, 2 H, 15'-CH_2), 1.65 (m, 2 H, 2'-CH_2-), 1.87 (m, 2 H, 6-CH_2-), 3.21 (t, J = 6 Hz, 2 H, 1'-CH_2-), 3.81 (t, J = 8 Hz, 2 H, 5-H), 6.09 (s, 2 H, -OCH_2O-), 6.44 (s, 2 H, -OCH_2O-), 6.94 (s, 1 H, 4-Ar-H), 7.58 (s, 1 H, 1-Ar-H), 7.84 (2 H, 11-Ar-H, 12-Ar-H), 8.55 (s, 1 H, 13-Ar-H) (Supplementary Fig. S1, S2 and Table 1). Yield: 38.2%. Mass spectrum (ESI): Calculated for $C_{35}H_{47}NO_4^+$ ($[M+H]^+$): 545.34, Found: 545.60 (Fig. 1C).

3.2. CCOP inhibited cancer cell viability

The cell viability was determined by MTT assay. Treatment with CCOP resulted in a dose- and time-dependent cytotoxicity in different cancer cells. The IC_{50} values were 2.12 μg/mL and 1.05 μg/mL against A549 cells at 24 h and 48 h, respectively. To identify whether the cytotoxicity of CCOP was specific to A549 cells, other cancer cell lines were used. Interestingly, similar results were observed in BGC-823, MDA-MB-231, HCT-116 and HepG2 cells (Fig. 2A). It was further showed that CCOP induced cell morphology shrinkage and detachment under a 2 μg/mL treatment (Fig. 2B). Moreover, the clonogenic assay performed with a continuing treatment of CCOP for 2 weeks showed markedly inhibitory effect on A549 cell growth (Fig. 2C). These data validated that CCOP could inhibit proliferation of cancer cells.

3.3. CCOP induced apoptosis in A549 cells

To identify whether CCOP-induced cytotoxicity was due to apoptosis induction, we employed Annexin-V/PI staining. The results showed that a significant apoptosis rate was induced by CCOP. Especially, the percentage of apoptotic cells was increased to 29.58% ($p < 0.01$) in cells treated with 2 μg/mL CCOP (Fig. 3A). In Hoechst 33342 staining, CCOP induced apoptotic cells with condensed and fragmented nucleus in A549 cells (Supplementary Fig. S3). Additionally, the AO/EB assay also revealed an increase in the number of red-stained dying cells and decreased number of green-stained healthy cells, confirmed that CCOP could induce apoptosis in A549 cells (Fig. 3B). Decreased MMP may be an early event in the process of apoptosis. Therefore, we further investigated the effect of CCOP on MMP. As expected, CCOP decreased the MMP in a dose-dependent manner. Compared with control, CCOP

(0.25−2 μg/mL) increased the percentage of cells with low MMP to 19.33%, 22.70%, 26.03% ($p < 0.05$) and 34.37% ($p < 0.01$), respectively (Fig. 3C), suggesting CCOP-induced apoptosis in A549 cells is associated with MMP disruption.

3.4. Effect of CCOP on apoptosis-related proteins

The mechanism of CCOP-induced apoptosis was explored by examining the expression of apoptosis-related proteins. Interestingly, western blot analysis showed that CCOP reduced the expression of anti-apoptotic Bcl-2 and increased the level of pro-apoptotic Bax (Fig. 4A). This observation confirmed the MMP disruption in CCOP incubated A549 cells. A modulation of Bcl-2 family proteins could activate caspase-dependent apoptosis [30]. To investigate the participation of caspase 3 and 9 in the pro-apoptotic effect of CCOP in the A549 cells, we measured the expression of these proteins after the cells exposed to the CCOP treatment. As shown in Fig. 4A, CCOP incubation increased the expression of cleaved caspases 3 and 9 in a dose-dependent manner. In addition, CCOP reduced the expression of upstream Pi3k and p-Akt signaling (Fig. 4B). These observations suggested that CCOP induced caspase-dependent apoptosis in A549 cells.

3.5. CCOP induced G0/G1 arrest in A549 cells

We also detected the effect of CCOP on cell cycle by flow cytometry. The results showed that CCOP induced G0/G1 arrest in A549 cells. Compared with control, CCOP increased the population of G0/G1 phase by 16.44%, 17.61% and 16.01% ($p < 0.05$) at the concentrations of 0.5−2 μg/mL, respectively, accompanied by a decrease in S phase cells ($p < 0.05$). However, CCOP had no influence on G2/M phase (Fig.

5A). During G0/G1 phase, CDKs and Cyclin D/E promote DNA replication and initiate G1-to-S transition [10]. Therefore, we further examined the expression of G0/G1 regulatory proteins. Relative to control, CCOP dose-dependently decreased the expression of CDKs 2, 4 and 6, Cyclins D and E (Fig. 5B). The results supported that CCOP could induce G0/G1 cell cycle arrest in A549 cells.

3.6. CCOP inhibited tumor growth *in vivo*

We further investigated whether CCOP could inhibit tumor growth in xenograft nude mice. As shown in Table 2, the gain in body weight was significantly decreased between TC and NC group ($p < 0.01$) at the end of the experiment, probably due to the cancer cell inoculation. On the other hand, the body weight of CCOP treated mice was not markedly different from those in TC and COP treated group ($p > 0.05$). Similarly, the organ index among all groups showed no obvious variation, indicated that CCOP is relatively safe *in vivo*. As shown in Fig. 6A and 6B, CCOP inhibited tumor growth in A549 xenograft nude mice. After 25 days, treatment with CCOP significantly decreased tumor weight by 19.0% ($p < 0.05$) and 58.2% ($p < 0.01$) in CCOP-L (5 mg/kg) and CCOP-H (10 mg/kg) groups respectively, as compared to TC. While high dose of COP (100 mg/kg) decreased only 7.9% of tumor weight compared to TC (Fig. 6C). Markedly, western blot analysis revealed that CCOP increased the expression of cleaved caspase 3, Bax and decreased Bcl-2 expression in tumor tissues (Fig. 6D). Immunohistochemical analysis (Fig. 6E) showed that, when compared with TC, CCOP-H decreased Ki-67 and Bcl-2 expression by 73.94% ($p < 0.01$) and 63.11% ($p < 0.05$), while increasing cleaved caspase 3 expression by 184.45% ($p < 0.01$). This

result supports the idea of apoptosis activation. However, the effect of COP was not significant ($p > 0.05$). These data indicated that CCOP could effectively block the progression of lung cancer *in vivo* and its anticancer effect was much better than that of COP.

4. Discussion

Lung cancer is the most common malignancy worldwide, with a high risk of metastasis and poor prognoses [31, 32], making the development of effective therapies for lung cancer an urgency. Preliminary results showed that CCOP significantly inhibited the proliferation of A549 and other cancer cell lines *in vitro*. Further studies indicated that the inhibitory effect was due to the apoptosis induction and G0/G1 cell cycle arrest. Rao *et al*. reported that COP inhibited A549 cell growth at IC_{50} value of 18.09 μM and induced G2/M cell cycle arrest [15]. However, the IC_{50} value of CCOP was 1.49–2.56 μg/mL, about ten-fold lower than that of COP in other cancer cell lines (IC_{50} > 27.13 μg/mL) [15, 16, 19, 33]. These results could be explained by the introduction of a long alkyl chain, which may enhance the compound lipophilicity.

Many cellular signals for life and death are regulated by Bcl-2 family proteins [34]. For example, Bcl-2 restrains MOMP and suppresses apoptosis [35]. Bax and Bcl-2 homologous antagonist/killer (Bak) undergo oligomerization to form a channel that triggers the release of apoptotic factors [36]. In addition, a decrease in MMP causes MOMP and mitochondria-dependent apoptotic pathway [34]. In this study, CCOP treatment significantly decreased MMP and Bcl-2 expression. On the other hand, the

treatment activated Bax, caspase 3 and 9 indicated that CCOP could induce mitochondria dysfunction and activate apoptosis in A549 cells.

It has been reported that the abnormal activation of Pi3k/Akt pathway is associated with tumorigenesis, apoptosis and metastasis [37], and inhibition of Akt phosphorylation stimulates caspase-meditated apoptosis in malignancies including lung cancer [38]. Our data revealed that CCOP markedly decreased the expression of p-Akt and the upstream regulator Pi3k in a dose-dependent manner, suggesting that CCOP might modulate the Pi3k/Akt signaling in A549 cells. P-Akt also regulates the cell division cycle and initiates G1-to-S phase transition which is regulated by the activation of cyclins (e.g. cyclins D and E) and CDKs (e.g. CDKs 2, 4 and 6) [10]. In this study, CCOP reduced the expression of cyclins D and E, and consistently decreased the expression of CDKs 2, 4 and 6. These data indicated that CCOP-induced apoptosis in A549 cells was associated with the suppression of Pi3k/Akt pathway.

Previous results from our lab showed that COP at a dose of 100 mg/kg significantly inhibited colon tumor growth [16, 17]. However, it showed only a 7.9% inhibition in A549 xenograft nude mice, probably due to the different types of cancer cells. In this study, although the dose of CCOP (10 mg/kg) was only one-tenth of COP's dose, it showed 58.2% inhibition rate, almost 7-fold compared to COP. These results further suggested that the anticancer activity of CCOP was more efficient than that of COP *in vivo*. In the progression of cancer development, the metastasis causes major death [39]. However, because of the tumor model, there was not observed metastasis in this study.

Nevertheless, in a mouse 4T1 spontaneous metastasis model, CCOP inhibited lung metastasis *in vivo* (Supplementary Fig. S4). Together, these data suggest that CCOP could block the progression of lung cancer.

5. Conclusion

In conclusion, we demonstrated that CCOP exerted anticancer activity by inducing mitochondria-dependent apoptosis and G0/G1 cell cycle arrest in A549 cells (Fig. 7). CCOP might be a potential candidate for lung cancer treatment. However, further clinical trials are needed to support our viewpoint. Besides, our data also provided evidences for the antitumor structural modification of COP.

Conflict of Interest

The authors declare no conflicts of interest.

Acknowledgments

This work was supported by The National Key Research and Development Program of China for Traditional Chinese Medicine Modernization (2017YFC1702600, 2017YFC1702605); Chongqing postgraduate research and research innovation project (CYB18087); The National Key Research and Development Program of China for Chinese Veterinarian Medicine Modernization and Green Cultivation Technology (2017YFD0501504); The Special Program for Common and Key Technological Innovations of Key Industries in Chongqing (cstc2016zdcy-ztzx10001); Industrial Technology System Program for Traditional Chinese Herbs of Chongqing Municipal Agricultural Commission (2017[5]); the County-University cooperation Innovation Funds of Southwest University (SZ201703,

HZ201601); Construction Project of Key subjects of Traditional Chinese Medicine of the State Administration of Traditional Chinese Medicine of the People's Republic of China.

References

[1] F. Bray, J. Ferlay, I. Soerjomataram, R.L. Siegel, L.A. Torre, A. Jemal, Global cancer statistics 2018: GLOBOCAN estimates of incidence and mortality worldwide for 36 cancers in 185 countries, CA. Cancer J. Clin., (2018).

[2] H. Borghaei, L. Paz-Ares, L. Horn, D.R. Spigel, M. Steins, N.E. Ready, L.Q. Chow, E.E. Vokes, E. Felip, E. Holgado, F. Barlesi, M. Kohlhaufl, O. Arrieta, M.A. Burgio, J. Fayette, H. Lena, E. Poddubskaya, D.E. Gerber, S.N. Gettinger, C.M. Rudin, N. Rizvi, L. Crino, G.R. Blumenschein, Jr., S.J. Antonia, C. Dorange, C.T. Harbison, F. Graf Finckenstein, J.R. Brahmer, Nivolumab versus Docetaxel in Advanced Nonsquamous Non-Small-Cell Lung Cancer, New Engl. J. Med., 373 (2015) 1627-1639.

[3] J. Tao, J. Xu, F. Chen, B. Xu, J. Gao, Y. Hu, Folate acid-Cyclodextrin/Docetaxel induces apoptosis in KB cells via the intrinsic mitochondrial pathway and displays antitumor activity in vivo, Eur. J. Pharm. Sci., 111 (2018) 540-548.

[4] P. Yu, L. Shi, M. Song, Y. Meng, Antitumor activity of paederosidic acid in human non-small cell lung cancer cells via inducing mitochondria-mediated apoptosis, Chem. Biol. Interact., 269 (2017) 33-40.

[5] Thornberry N A, L. Y., Caspases: enemies within, Science, 281 (1998) 1312-1316.

[6] M. Brentnall, L. Rodriguez-Menocal, R.L. De Guevara, E. Cepero, L.H. Boise, Caspase-9, caspase-3 and caspase-7 have distinct roles during intrinsic apoptosis, BMC Cell Biol., 14 (2013) 32.

[7] S. Vyas, E. Zaganjor, M.C. Haigis, Mitochondria and Cancer, Cell, 166 (2016) 555-566.

[8] M. Martini, M.C. De Santis, L. Braccini, F. Gulluni, E. Hirsch, PI3K/AKT signaling pathway and cancer: an updated review, Ann. Med., 46 (2014) 372-383.

[9] J. Liang, J.M. Slingerland, Multiple roles of the PI3K/PKB (Akt) pathway in cell cycle progression, Cell Cycle, 2 (2003) 339-345.

[10] C. Bertoli, J.M. Skotheim, R.A. de Bruin, Control of cell cycle transcription during G1 and S phases, Nat. Rev. Mol. Cell Biol., 14 (2013) 518-528.

[11] M.H. Lee, Y. Cho, D.H. Kim, H.J. Woo, J.Y. Yang, H.J. Kwon, M.J. Yeon, M. Park, S.H. Kim, C. Moon, N. Tharmalingam, T.U. Kim, J.B. Kim, Menadione induces G2/M arrest in gastric cancer cells by down-regulation of CDC25C and proteasome mediated degradation of CDK1 and cyclin B1, Am. J. Transl. Res., 8 (2016) 5246-5255.

[12] I.A. Mayer, C.L. Arteaga, The PI3K/AKT Pathway as a Target for Cancer Treatment, Annu. Rev. Med., 67 (2016) 11-28.

[13] A. Nahata, A. Saxena, N. Suri, A.K. Saxena, V.K. Dixit, *Sphaeranthus indicus* induces apoptosis through mitochondrial-dependent pathway in HL-60 cells and exerts cytotoxic potential on several human cancer cell lines, Integr. Cancer Ther., 12 (2013) 236-247.

[14] D.A. Fuchs, R.K. Johnson, Cytologic evidence that taxol, an antineoplastic agent from *Taxus brevifolia*, acts as a mitotic spindle poison, Cancer Treat. Rep., 62 (1978) 1219.

[15] P.C. Rao, S. Begum, M. Sahai, D.S. Sriram, Coptisine-induced cell cycle arrest at G2/M phase and reactive oxygen species–dependent mitochondria-mediated apoptosis in non-small-cell lung cancer A549 cells, Tumor Biol, 39 (2017) 101042831769456.

[16] T. Huang, Y. Xiao, L. Yi, L. Li, M. Wang, C. Tian, H. Ma, K. He, Y. Wang, B. Han, X. Ye, X. Li, Coptisine from *Rhizoma coptidis* Suppresses HCT-116 Cells-related Tumor Growth in vitro and in vivo, Sci. Rep., 7 (2017) 38524.

[17] B. Han, P. Jiang, Z. Li, Y. Yu, T. Huang, X. Ye, X. Li, Coptisine-induced apoptosis in human colon cancer cells (HCT-116) is mediated by PI3K/Akt and mitochondrial-associated apoptotic pathway, Phytomedicine, 48 (2018) 152-160.

[18] F.N. Chai, W.Y. Ma, J. Zhang, H.S. Xu, Y.F. Li, Q.D. Zhou, X.G. Li, X.L. Ye, Coptisine from *Rhizoma coptidis* exerts an anti-cancer effect on hepatocellular carcinoma by up-regulating miR-122, Biomed. Pharmacother., 103 (2018) 1002-1011.

[19] J. Li, D.M. Qiu, S.H. Chen, S.P. Cao, X.L. Xia, Suppression of Human Breast Cancer Cell Metastasis by Coptisine in Vitro, Asian. Pac. J. Cancer. Prev., 15 (2014) 5747-5751.

[20] D. Yu, S. Fu, Z. Cao, M. Bao, G. Zhang, Y. Pan, W. Liu, Q. Zhou, Unraveling the novel anti-osteosarcoma function of coptisine and its mechanisms, Toxicol. Lett., 226 (2014) 328-336.

[21] Yan. Y, Zhang. H, Zhang. Z, Song. J, Chen. Y, Wang. X, He. Y, Qin. H, Fang. L, Du. G, Pharmacokinetics and tissue distribution of coptisine in rats after oral administration by liquid chromatography–mass spectrometry, Biomed. Chromatogr., 31 (2016).

[22] X. Ye, K. He, X. Zhu, B. Zhang, X. Chen, J. Yi, X. Li, Synthesis and antihyperlipidemic efficiency of berberine-based HMG-CoA reductase inhibitor, Med. Chem. Res., 21 (2011) 1353-1362.

[23] Y. Hu, S. Fan, X. Liao, C. Chen, L. Su, X. Li, Pharmacokinetics, excretion of 8-cetylberberine and its main metabolites in rat urine, J. Pharm. Biomed. Anal., 132 (2016) 195-206.

[24] X.F. Jiang, X.G. Li, L. Tang, X.L. Ye, Synthesis and in vitro glucose-lowering effect of 8-alkyl-coptisine, Chin. Tradit. Herbal Drugs, 42 (2011) 640-644.

[25] X.F. Jiang, X.L. Ye, B. Zhang, X.G. Li, X. Liu, Synthesis and Antimicrobial Activity of 8-Alkyl Coptisine Derivatives, Asian J. Chem., 23 (2011) 3849-3852.

[26] H.Y. Chen, X.L. Ye, X.L. Cui, K. He, Y.N. Jin, Z. Chen, X.G. Li, Cytotoxicity and antihyperglycemic effect of minor constituents from *Rhizoma coptis* in HepG2 cells, Fitoterapia, 83 (2012) 67-73.

[27] K.W. Zeng, X.M. Wang, H. Ko, H.C. Kwon, J.W. Cha, H.O. Yang, Hyperoside protects primary rat cortical neurons from neurotoxicity induced by amyloid beta-protein via the PI3K/Akt/Bad/Bcl(XL)-regulated mitochondrial apoptotic pathway, Eur. J. Pharmacol., 672 (2011) 45-55.

[28] H. Chang, H. Huang, T. Huang, P. Yang, Y. Wang, H. Juan, Flow Cytometric

Detection of Mitochondrial Membrane Potential, Bio-protocol,, 3 (2013).

[29] M. Wang, H. Ma, C. Tian, S. Liu, X. Ye, D. Zhou, Y. Li, N. Hui, X. Li, Bioassay-guided isolation of glycoprotein SPG-56 from sweet potato Zhongshu-1 and its anti-colon cancer activity in vitro and in vivo, J. Funct. Foods, 35 (2017) 315-324.

[30] C.C. Wu, S.E. Lee, S. Malladi, M.D. Chen, N.J. Mastrandrea, Z.W. Zhang, S.B. Bratton, The Apaf-1 apoptosome induces formation of caspase-9 homo- and heterodimers with distinct activities, Nat. Commun., 7 (2016) 13565.

[31] R.L. Siegel, K.D. Miller, A. Jemal, Cancer statistics, 2016, CA. Cancer J. Clin., 66 (2016) 7-30.

[32] M. Riihimaki, A. Hemminki, M. Fallah, H. Thomsen, K. Sundquist, J. Sundquist, K. Hemminki, Metastatic sites and survival in lung cancer, Lung cancer, 86 (2014) 78-84.

[33] F.N. Chai, J. Zhang, H.M. Xiang, H.S. Xu, Y.F. Li, W.Y. Ma, X.G. Li, X.L. Ye, Protective effect of Coptisine from *Rhizoma coptidis* on LPS/D-GalN-induced acute liver failure in mice through up-regulating expression of miR-122, Biomed. Pharmacother., 98 (2017) 180-190.

[34] S.W. Tait, D.R. Green, Mitochondria and cell death: outer membrane permeabilization and beyond, Nat. Rev. Mol. Cell Biol., 11 (2010) 621-632.

[35] T. Moldoveanu, A.V. Follis, R.W. Kriwacki, D.R. Green, Many players in BCL-2 family affairs, Trends Biochem. Sci., 39 (2014) 101-111.

[36] S. Iyer, K. Anwari, A.E. Alsop, W.S. Yuen, D.C. Huang, J. Carroll, N.A. Smith, B.J. Smith, G. Dewson, R.M. Kluck, Identification of an activation site in Bak and

mitochondrial Bax triggered by antibodies, Nat. Commun., 7 (2016) 11734.

[37] N.B. Hao, B. Tang, G.Z. Wang, R. Xie, C.J. Hu, S.M. Wang, Y.Y. Wu, E. Liu, X. Xie, S.M. Yang, Hepatocyte growth factor (HGF) upregulates heparanase expression via the PI3K/Akt/NF-kappaB signaling pathway for gastric cancer metastasis, Cancer Lett., 361 (2015) 57-66.

[38] S.C. Tripathi, J.F. Fahrmann, M. Celiktas, M. Aguilar, K.D. Marini, M.K. Jolly, H. Katayama, H. Wang, E.N. Murage, J.B. Dennison, D.N. Watkins, H. Levine, E.J. Ostrin, A. Taguchi, S.M. Hanash, MCAM Mediates Chemoresistance in Small-Cell Lung Cancer via the PI3K/AKT/SOX2 Signaling Pathway, Cancer Res., 77 (2017) 4414-4425.

[39] X. Zhuang, H. Zhang, X. Li, X. Li, M. Cong, F. Peng, J. Yu, X. Zhang, Q. Yang, G. Hu, Differential effects on lung and bone metastasis of breast cancer by Wnt signalling inhibitor DKK1, Nat. Cell Biol., 19 (2017) 1274.

Table 1. ^{1}H NMR and ^{13}C NMR spectra of CCOP (400 MHz, CD_3OD).

NO.	δ_H	δ_C
1	7.58 (1 H, s)	106.84
2		151.88
3		161.76
4	6.94 (1 H, s)	108.68
4a		131.86
5	3.81 (2 H, t, *J* = 8 Hz)	28.28
6	1.87 (2 H, m)	50.97
8		149.74
8a		115.28
9		145.89
10		149.88
11	7.84 (1 H, s) (overlap)	121.47
12	7.84 (1 H, s) (overlap)	124.24
12a		134.07
13	8.55 (1 H, s)	122.91
13a		139.49
13b		121.77
$-OCH_2O-$	6.09 (2 H, s)	103.57
$-OCH_2O-$	6.44 (2 H, s)	104.96
1'	3.21 (2 H, t, *J* = 6 Hz)	33.35
2'	1.65 (2 H, m)	33.06
3'	1.29 (2 H, m) (overlap)	29.27
4'	1.29 (2 H, m) (overlap)	30.25
5'	1.29 (2 H, m) (overlap)	30.45
6'	1.29 (2 H, m) (overlap)	30.61
7'	1.29 (2 H, m) (overlap)	30.69
8'-13'	1.29 (12 H, m) (overlap)	30.74 (overlap)
14'	1.29 (2 H, m) (overlap)	30.77
15'	1.46 (2 H, m)	23.71
16'	0.90 (3 H, t, *J* = 6 Hz)	14.41

Data were detected on a Bruker Ascend 400 spectrometer, chemical shifts (δ) were expressed in ppm.

Table 2. Effects of CCOP on body weight and organ index (%) in BALB/c nude mice.

Groups	Body weight (g)		Heart (%)	Liver (%)	Spleen (%)	Lung (%)	Kidneys (%)
	Beginning	End					
NC	14.90 ± 0.59	22.96 ± 1.22	0.62 ± 0.12	6.05 ± 0.70	0.54 ± 0.08	0.70 ± 0.04	1.75 ± 0.11
TC	14.71 ± 0.60	19.64 ± 0.85**	0.64 ± 0.05	6.63 ± 0.26	0.53 ± 0.10	0.74 ± 0.04	1.80 ± 0.19
COP	14.91 ± 0.37	19.12 ± 0.46	0.65 ± 0.08	6.48 ± 0.39	0.58 ± 0.07	0.70 ± 0.06	1.73 ± 0.08
CCOP-L	15.09 ± 0.57	19.05 ± 1.56	0.64 ± 0.03	6.23 ± 0.60	0.60 ± 0.12	0.69 ± 0.04	1.81 ± 0.20
CCOP-H	14.74 ± 0.31	18.64 ± 0.98	0.71 ± 0.10	6.36 ± 0.50	0.58 ± 0.10	0.73 ± 0.07	1.88 ± 0.16

Organ index = weight of organ / body weight × 100%.

Data were presented as mean ± SD, n = 5. **$p < 0.01$ compared with NC group. NC, normal control; TC, tumor control. COP, coptisine at a dosage of 100 mg/kg; CCOP-L, CCOP at low dosage (5 mg/kg); CCOP-H, CCOP at high dosage (10 mg/kg).

Figure captions

Scheme 1. Synthetic route of CCOP (R = $-CH_2-(CH_2)_{14}-CH_3$).

Fig. 1. Chemical structure and identification of CCOP. (A) Chemical structure. (B) HPLC analysis. HPLC detection condition: Polaris 5 C18-A column (250 × 10.0 mm); mobile phase, methanol : water (0.05% triethylamine, 0.1% phosphoric acid) = 87:13; flow rate, 1 mL/min; injection volume, 10 μL; detection wavelength, 347 nm; column temperature, 30ºC. (C) Mass spectra (ESI). Calculated for $C_{35}H_{47}NO_4^+$ ($[M+H]^+$): 545.34, Found: 545.60.

Fig. 2. Effects of CCOP on cancer cell viability. (A) Cells were treated with CCOP (0−4 μg/mL) for 24 h or 48 h, and determined by MTT assay. Data were presented as mean ± SD, n = 5. (B) Morphology of A549 cells treated with CCOP (0−2 μg/mL) for 24 h. Scale bar, 200 μm. (C) Colonies of A549 cells treated with CCOP (0−2 μg/mL) for 2 weeks. The picture depicts the crystal violet-stained colonies and the cloning efficiency compared with control. Data were presented as mean ± SD, n = 3. *p < 0.05 and **p < 0.01 compared with control.

Fig. 3. Effects of CCOP on apoptosis in A549 cells. (A) Cells were treated with CCOP (0−2 μg/mL) for 24 h, the apoptotic cells were stained by Annexin-V/PI and analyzed by flow cytometry. (B) Cells were resuspended in PBS and incubated with AO/EB (4 μg/mL) for 1 min in darkness. The arrows indicate typical cell bodies (healthy cell, green-stained; apoptotic cell, red-stained). Scale bar, 100 μm. Data were presented as mean ± SD, n = 3. *p < 0.05 and **p < 0.01 compared with control. (C) Cells were treated with CCOP (0−2 μg/mL) for 24 h, stained with $DiOC_6(3)$ and

measured by flow cytometry. Cells with lower fluorescence indicate loss of MMP. Data were presented as mean ± SD, n = 3. $^{**}p < 0.01$ compared with control

Fig. 4. Effects of CCOP on apoptosis related proteins in A549 cells. Cells were treated with CCOP (0−2 μg/mL) for 24 h. The expression of apoptosis related proteins (A) Bcl-2, Bax, cleaved caspase 3 and 9 (B) Pi3k, Akt and p-Akt was determined by western blot. Data were presented as mean ± SD, n = 3. $^{*}p < 0.05$ and $^{**}p < 0.01$ compared with control.

Fig. 5. Effects of CCOP on cell cycle in A549 cells. (A) Cells were treated with CCOP (0−2 μg/mL) for 24 h, then, stained with PI and analyzed by flow cytometry. Data were presented as mean ± SD, n = 3. $^{*}p < 0.05$ and $^{**}p < 0.01$ compared with control. (B) The expression of cell cycle related proteins (CDK 2, CDK 4, CDK 6, Cyclin D and Cyclin E) was determined by western blot. Data were presented as mean ± SD, n = 3. $^{*}p < 0.05$ and $^{**}p < 0.01$ compared with control.

Fig. 6. Effects of CCOP on tumor growth *in vivo*. BALB/c nude mice were subcutaneously injected with A549 cells into the right armpit and orally administered with CCOP or COP every day. (A) Image of excised tumors. (B) Tumor volume. (C) Tumor weight. Data were presented as mean ± SD, n = 5. $^{*}p < 0.05$ and $^{**}p < 0.01$ compared with TC group. (D) Western blot and (E) immunohistochemistry analysis of apoptosis related proteins in tumor tissue. Scale bars, 100 μm. Data were presented as mean ± SD, n = 3. $^{*}p < 0.05$ and $^{**}p < 0.01$ compared with TC group. TC, tumor control; COP, COP at a dosage of 100 mg/kg; CCOP-L, CCOP at low dosage (5 mg/kg); CCOP-H, CCOP at high dosage (10 mg/kg).

Fig. 7. Proposed mechanism of CCOP in A549 lung cancer. CCOP inactivates Pi3k/Akt signaling pathway, decreases mitochondrial membrane potential and activates caspase-dependent apoptosis. Simultaneously, CCOP suppresses the expression of cyclin D, cyclin E and their corresponding CDK 2, CDK 4, CDK 6, resulting in G0/G1 cell cycle arrest.

Figures

Scheme 1.

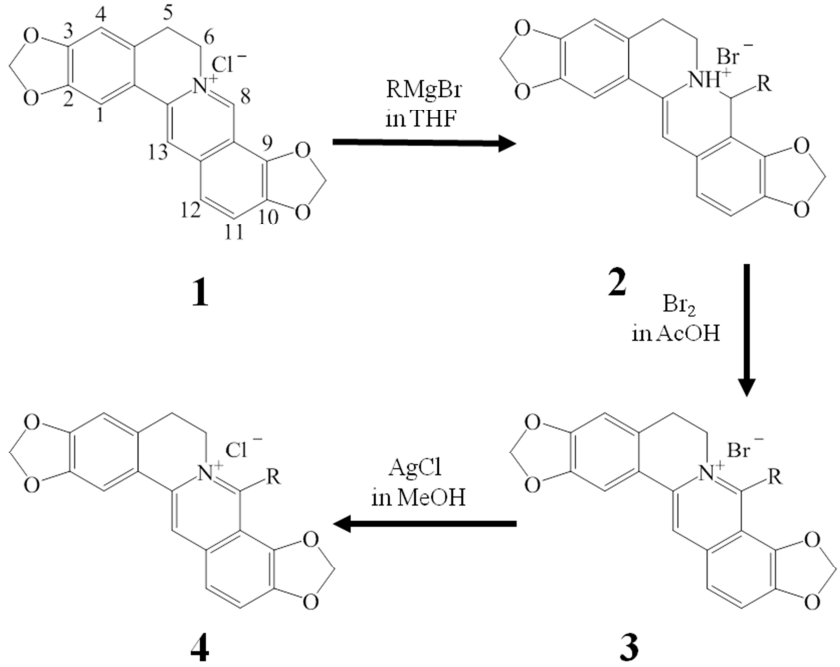

Fig. 1

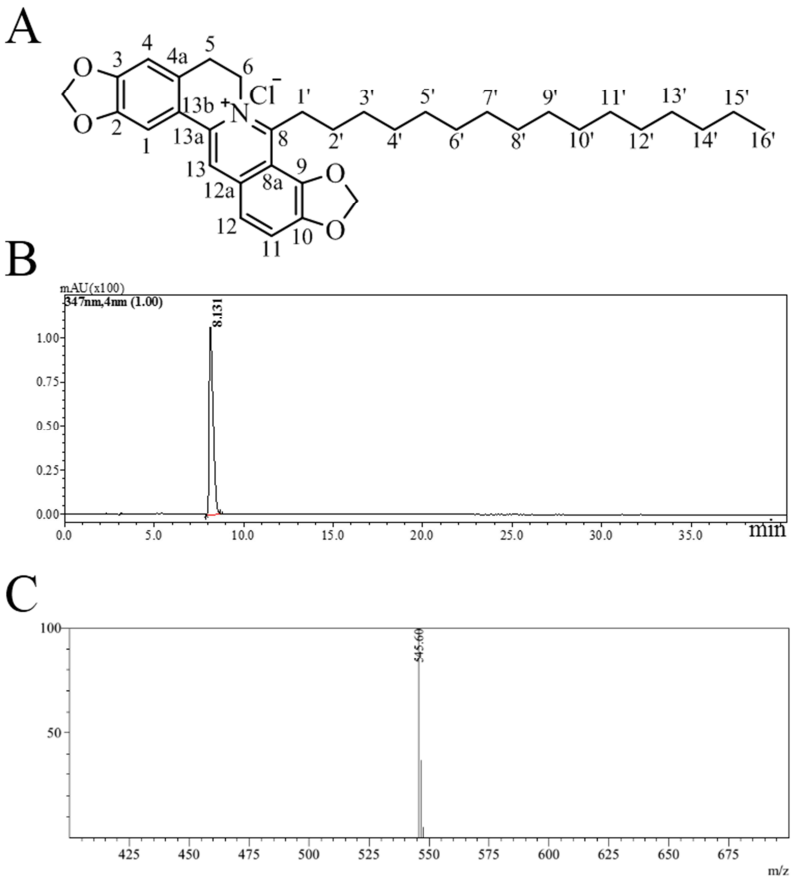

Fig. 2

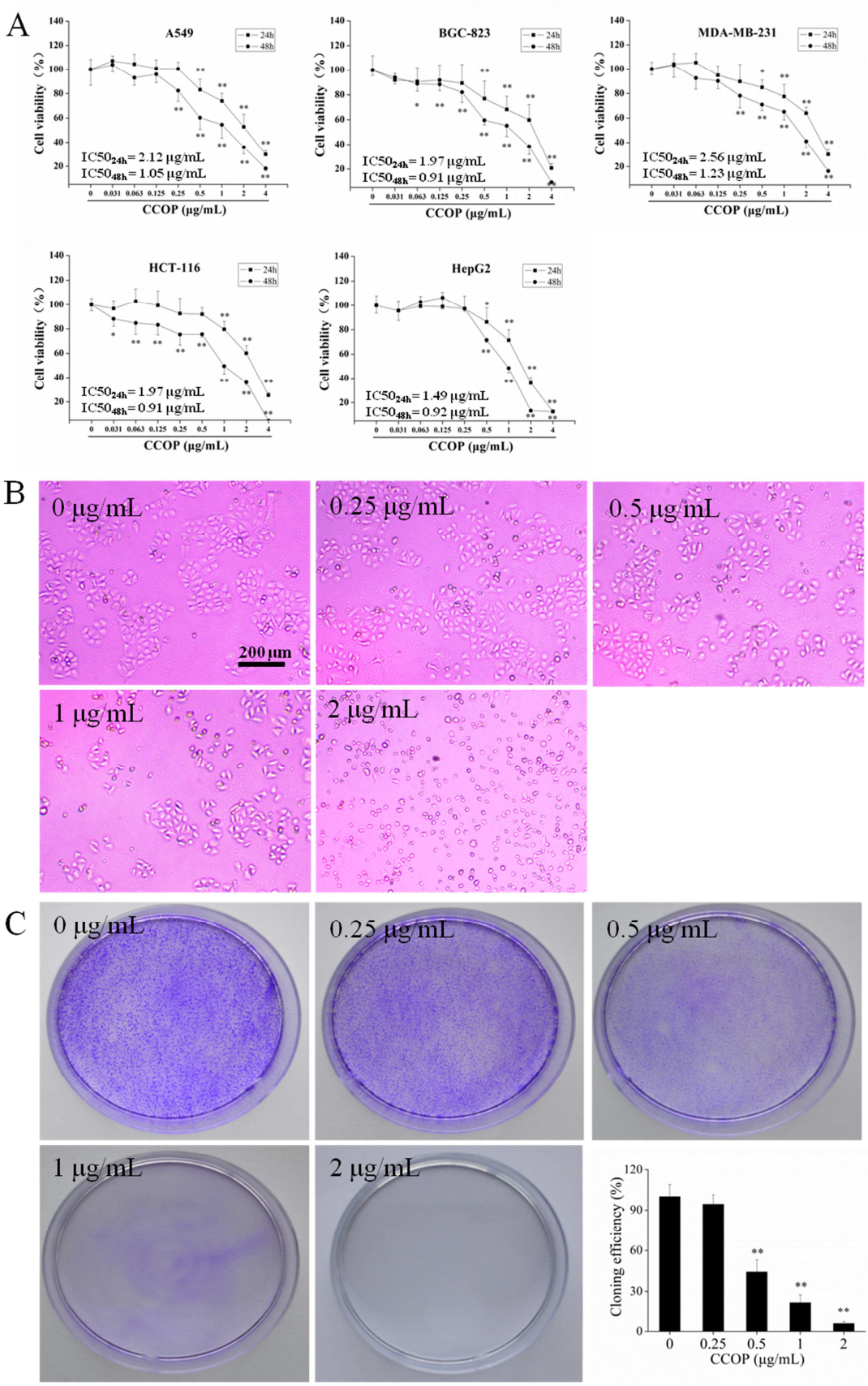
A
A549
BGC-823
MDA-MB-231
HCT-116
HepG2
24h
48h
Cell viability (%)
CCOP (μg/mL)
IC50$_{24h}$= 2.12 μg/mL
IC50$_{48h}$= 1.05 μg/mL
IC50$_{24h}$= 1.97 μg/mL
IC50$_{48h}$= 0.91 μg/mL
IC50$_{24h}$= 2.56 μg/mL
IC50$_{48h}$= 1.23 μg/mL
IC50$_{24h}$= 1.97 μg/mL
IC50$_{48h}$= 0.91 μg/mL
IC50$_{24h}$= 1.49 μg/mL
IC50$_{48h}$= 0.92 μg/mL
B
0 μg/mL
0.25 μg/mL
0.5 μg/mL
1 μg/mL
2 μg/mL
200 μm
C
0 μg/mL
0.25 μg/mL
0.5 μg/mL
1 μg/mL
2 μg/mL
Cloning efficiency (%)
CCOP (μg/mL)

Fig. 3

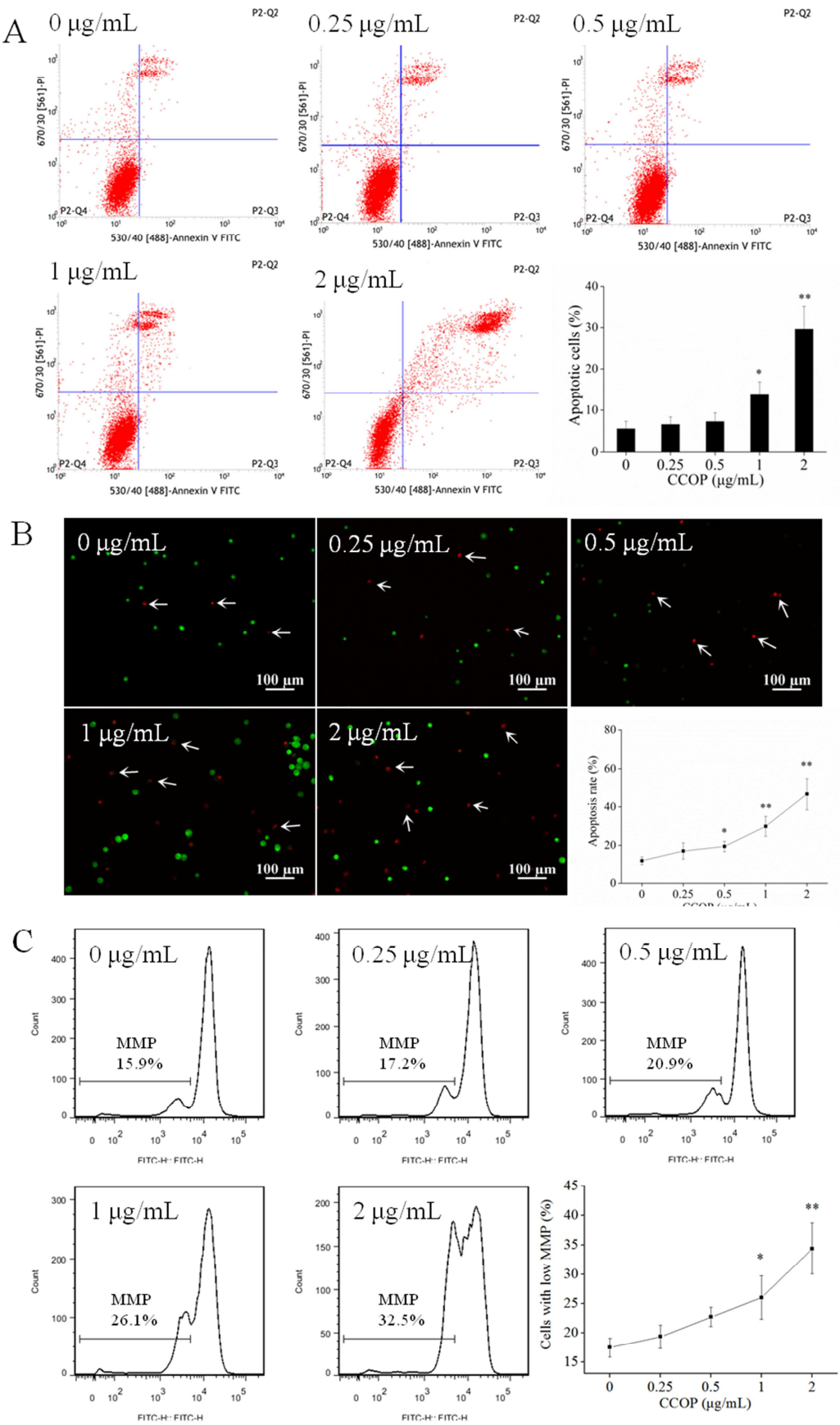
A
0 μg/mL
0.25 μg/mL
0.5 μg/mL
1 μg/mL
2 μg/mL
P2-Q2
P2-Q4
P2-Q3
670/30 [561]-PI
530/40 [488]-Annexin V FITC
Apoptotic cells (%)
CCOP (μg/mL)
B
100 μm
Apoptosis rate (%)
C
MMP
15.9%
17.2%
20.9%
26.1%
32.5%
Count
FITC-H : FITC-H
Cells with low MMP (%)
CCOP (μg/mL)

Fig. 4

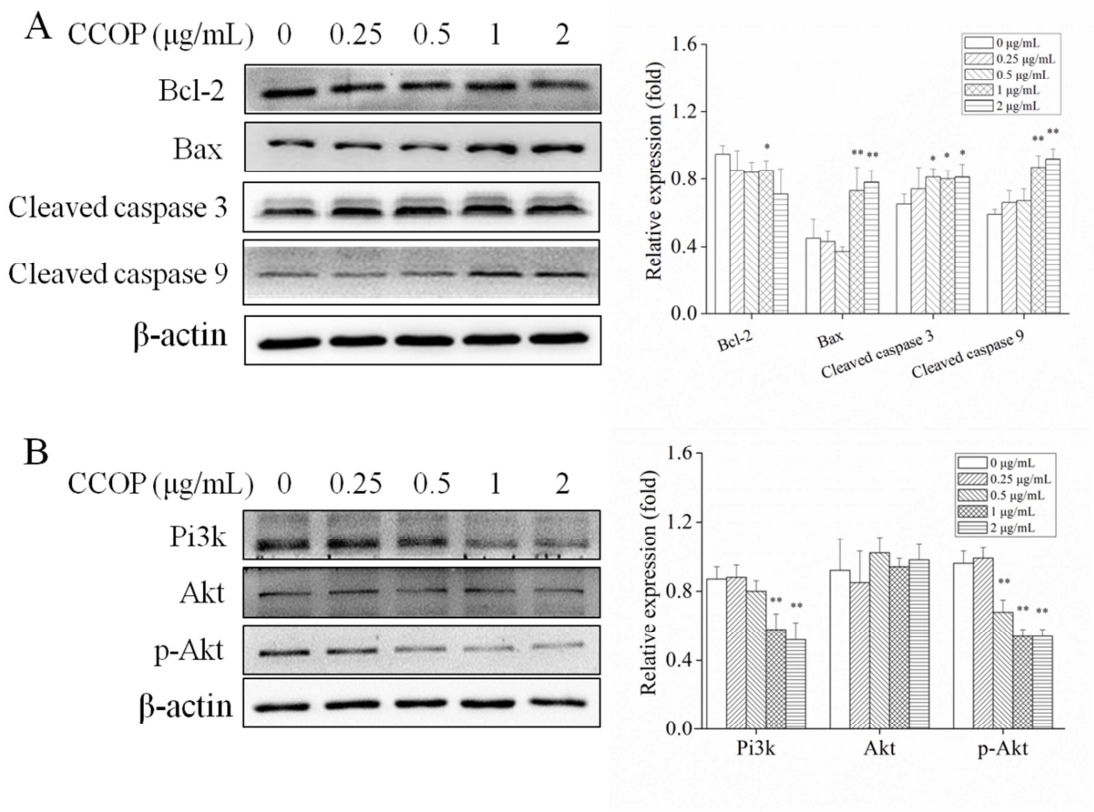

Fig. 5

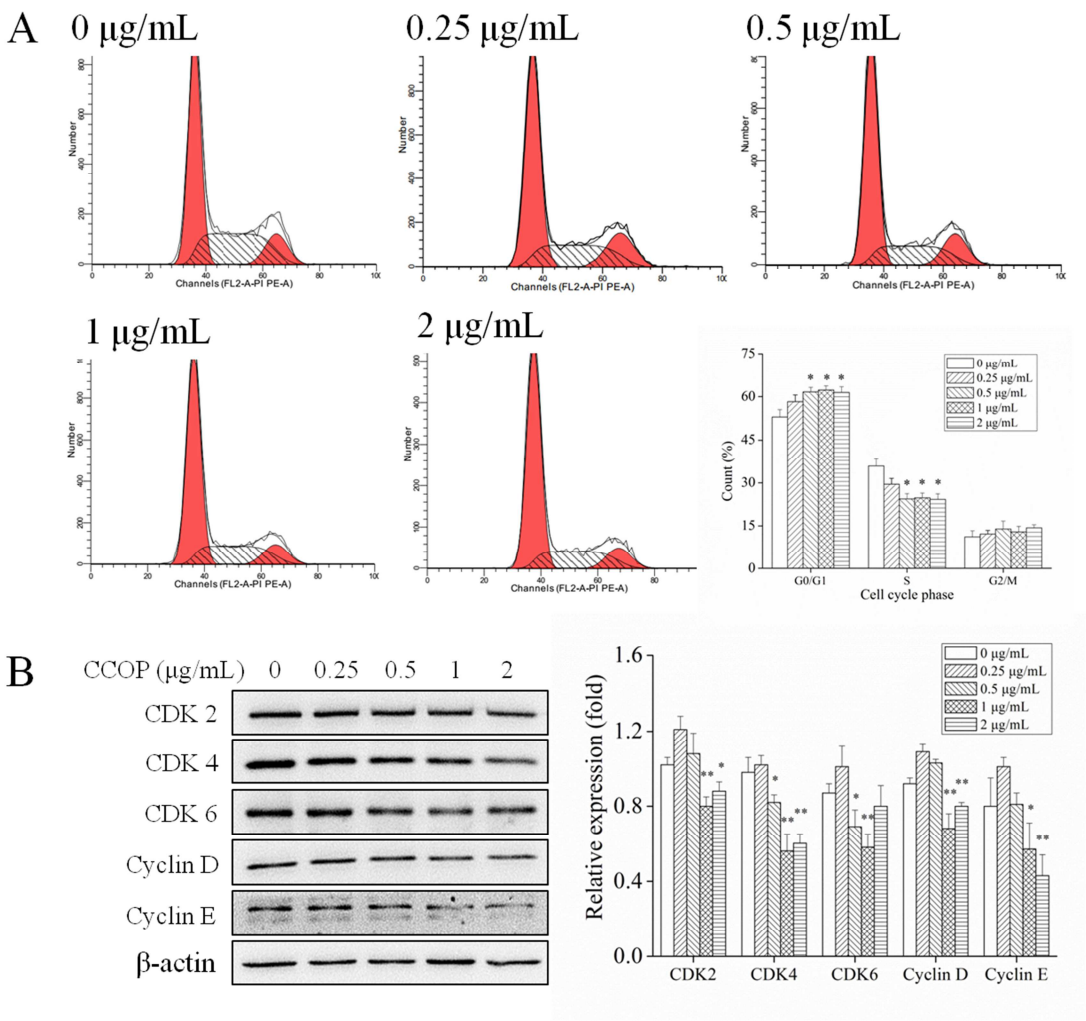

Fig. 6

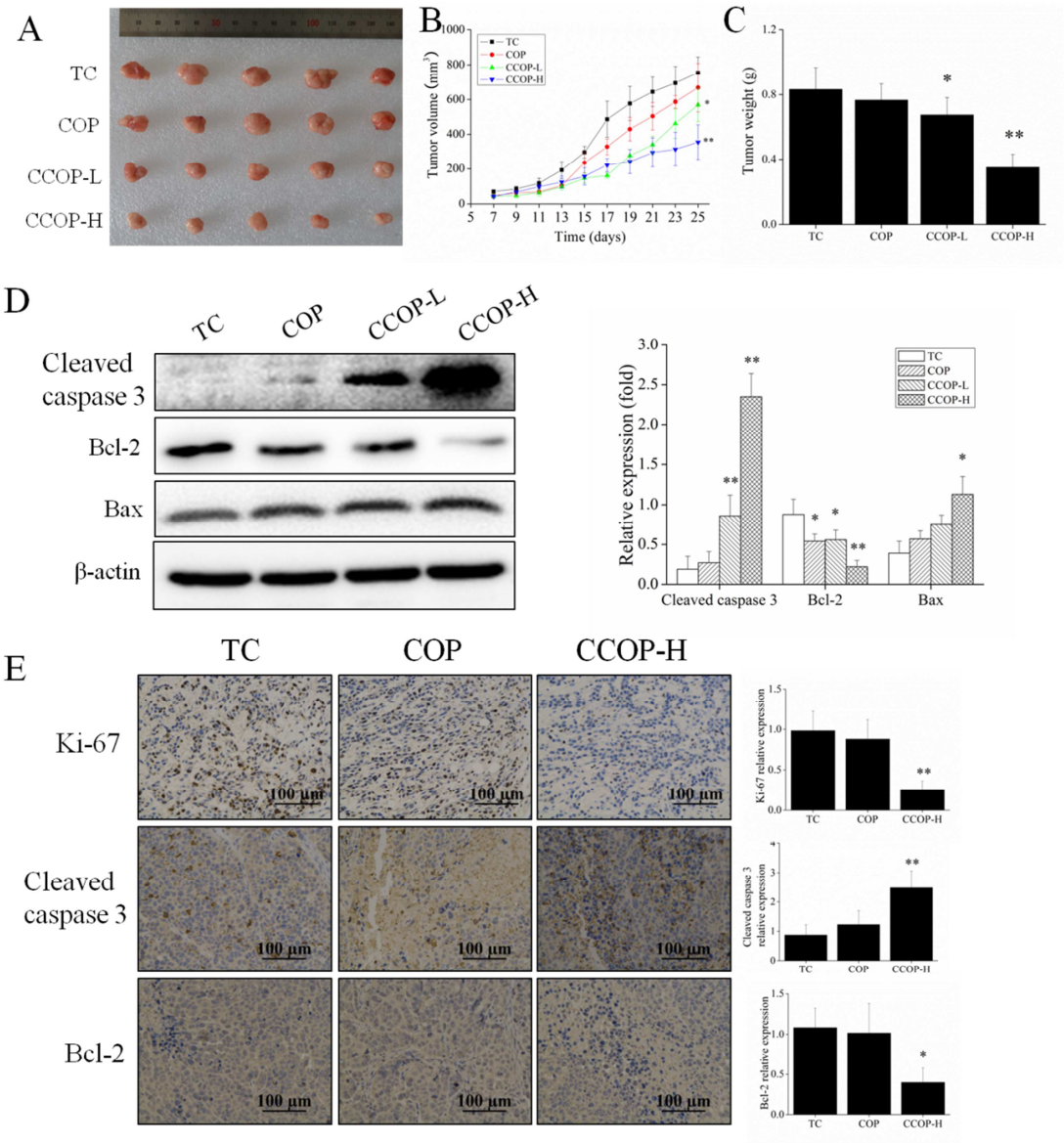
A
TC
COP
CCOP-L
CCOP-H
B
Tumor volume (mm³)
Time (days)
C
Tumor weight (g)
D
Cleaved caspase 3
Bcl-2
Bax
β-actin
Relative expression (fold)
E
Ki-67
Cleaved caspase 3
Bcl-2
100 μm

Fig. 7

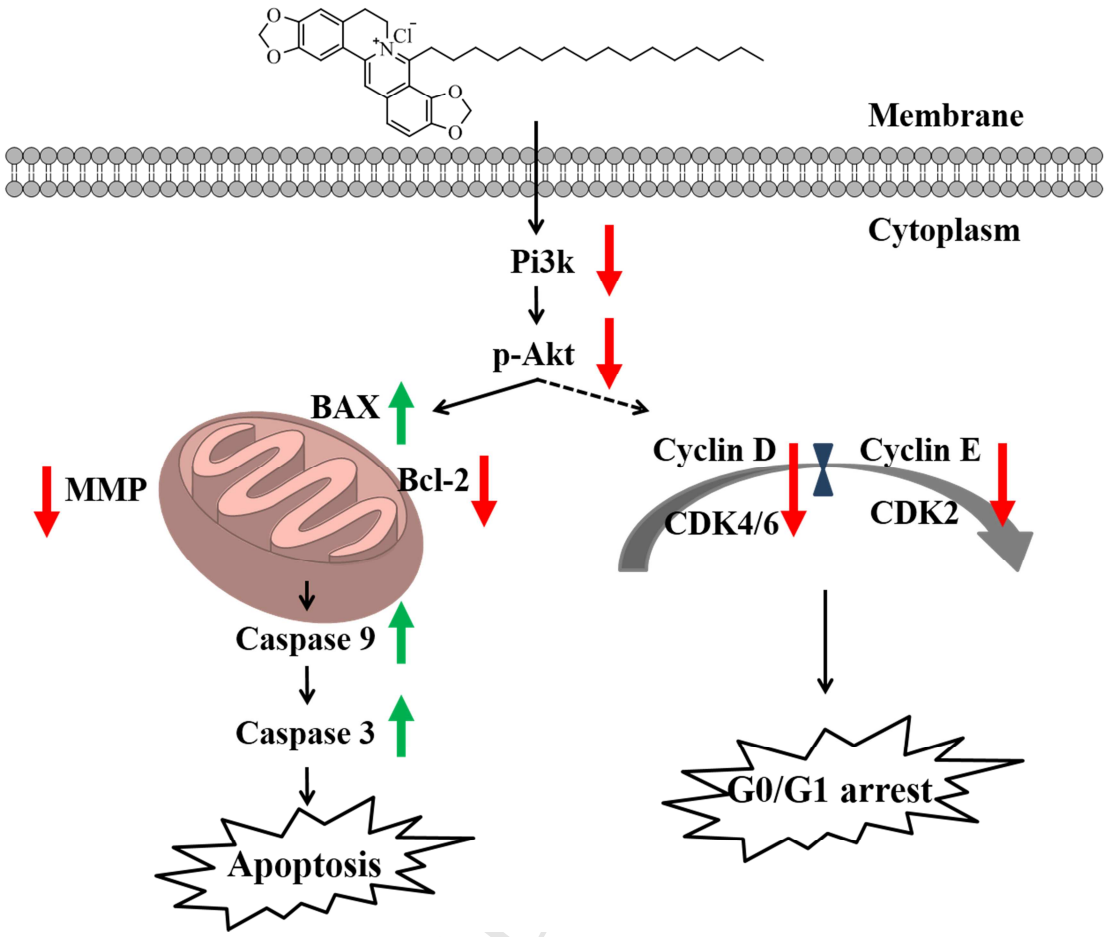

Highlights

1. A new coptisine derivative 8-cetylcoptisine is synthesized and characterized.
2. CCOP inhibits cell growth in A549 and other cancer cell lines.
3. CCOP induces mitochondria-dependent apoptosis and G0/G1 arrest in A549 cells.
4. CCOP exhibits better antitumor effect than COP in A549 xenograft nude mice.